Iron Losses in a Medium-Frequency Transformer Operated in a High-Power DC–DC Converter

Nils Soltau,[1] Daniel Eggers,[2] Kay Hameyer,[2] and Rik W. De Doncker[1]

[1]Institute for Power Generation and Storage Systems, E.ON Energy Research Center, RWTH Aachen University, Aachen D-52074, Germany

[2]Institute of Electrical Machines, RWTH Aachen University, Aachen D-52062, Germany

The three-phase dual-active bridge is a dc–dc converter, which is highly suitable for high-power applications. Among others, this is due to the medium-frequency transformer in the ac link, which provides galvanic isolation. The transformer is operated with a square-shaped voltage waveform. The flux density in the transformer core is piecewise linear. However, for the sake of simplicity, the magnetic flux is often assumed sinusoidal. Thereby, the actual iron losses generated in the core material are misinterpreted. This paper discusses the difference between the exact piecewise linear and the sinusoidal course in terms of iron losses. Silicon steel with a thickness of 0.18 mm is measured at a frequency of 1000 Hz, comparing the sinusoidal excitation with the actual one. The measurements are validated using the improved generalized Steinmetz equation. Finally, the transformer core losses are evaluated when the dc–dc converter is operated under load. The results are confirmed through measurement.

***Index Terms*—DC–DC power converters, loss measurement, magnetic hysteresis, power transformer losses, power transformers, soft magnetic materials.**

I. Introduction

THE three-phase dual-active bridge (DAB3), as shown in Fig. 1, is a dc–dc converter, which is especially suitable for high-power applications [1]. Its inherent soft-switching capability reduces the switching losses drastically and leads to a high efficiency of the converter. The three-phase transformer in the ac link provides galvanic isolation, which is often essential in high-power applications for safety reasons and to prevent common-mode currents [2]. In addition, an arbitrary dc–dc voltage conversion ratio can be set by an appropriate winding ratio of the transformer.

The three-phase transformer is operated at elevated frequencies, to achieve a high power density and reduce the core losses. In this paper, the rated power of the dc–dc converter is 5 MW. The switching frequency of the semiconductor switches and with it the fundamental frequency of the flux in the transformer is $f = 1$ kHz. The primary and secondary side dc voltages are $U_{\mathrm{pDC}} = U_{\mathrm{sDC}} = 5$ kV.

In a DAB3, the input and output bridges generate a six-step waveform, as shown in Fig. 2. Power is transferred by introducing a phase shift between the input and output bridges, where the output bridge is lagging by the so-called load angle φ. Due to the voltage difference across the stray inductance L_σ of the transformer, a current is built up in the ac link, leading to a power flow through the converter.

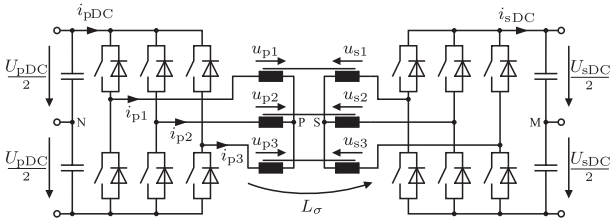

Fig. 1. Topology of a DAB3 dc–dc converter.

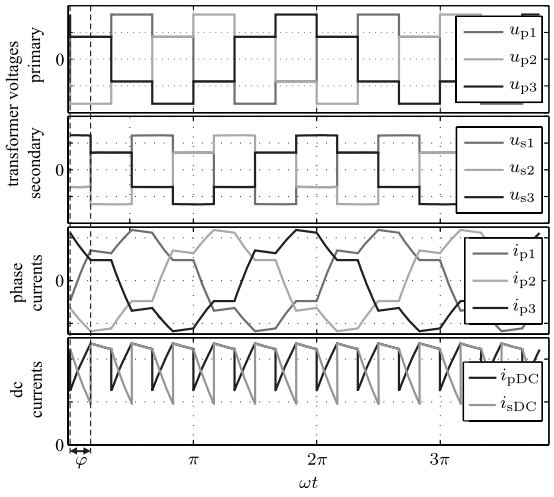

Fig. 2. Characteristic waveforms in a DAB3.

II. Operation of the Medium-Frequency Transformer

The phase voltages at the transformer form a six-step waveform with the discrete values $\pm(2/3)U_{\mathrm{DC}}$, $\pm(1/3)U_{\mathrm{DC}}$, as shown in Fig. 2. According to the main inductance L_m of the transformer, a magnetizing current is built up leading to a magnetic flux in the transformer core. Neglecting the stray inductance of the transformer, the course of the magnetic flux is piecewise linear, corresponding to the integral of the phase voltage. In the following, measurements on silicon steel core material are conducted and the difference between sinusoidal and piecewise linear excitation is investigated.

Manuscript received June 29, 2013; revised August 19, 2013; accepted September 24, 2013. Date of current version February 21, 2014. Corresponding author: N. Soltau (e-mail: nsoltau@eonerc.rwth-aachen.de).

Color versions of one or more of the figures in this paper are available online at http://ieeexplore.ieee.org.

Digital Object Identifier 10.1109/TMAG.2013.2283733

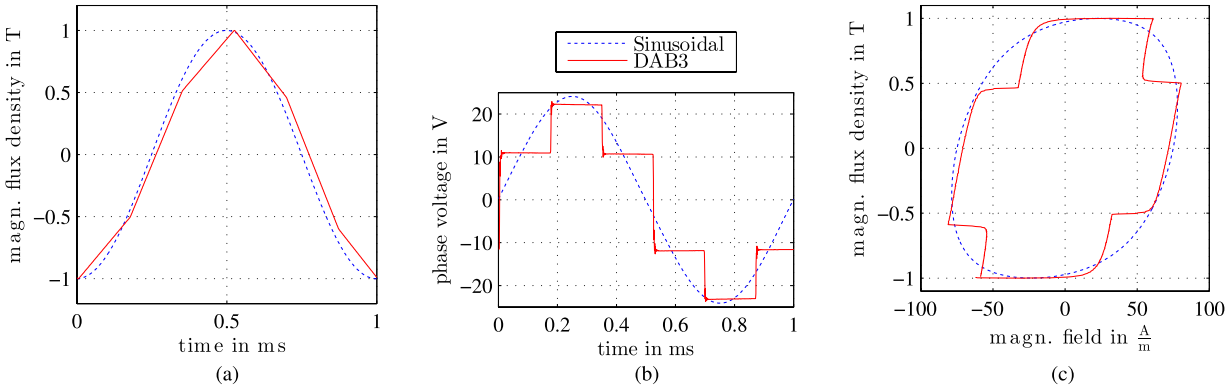

Fig. 3. Measuring results. (a) Magnetic flux density in the core material. (b) Compared transformer voltages. (c) Magnetic hysteresis loop.

III. Core Losses in a DAB3

A variety of research papers discuss the losses in core material exposed to nonsinusoidal excitation. Most of those papers deal with drive applications. The machines are operated with pulsewidth modulations [3]–[6] or fundamental frequency modulations [7] at frequencies of 50–60 Hz. Compared with that, the fundamental frequency in a DAB3 is one to two decades higher, involving additional core loss mechanism. Therefore, the core loss in a DAB3 is investigated further in the following.

To determine the transformer-core losses in a DAB3 application, measurements for frequencies up to 10 kHz of the laser-processed grain-orientated steel (thickness $d = 0.18$ mm) were performed with an Epstein frame at the Institute of Electrical Machines, RWTH Aachen University. The test bench allows the generation of an arbitrary form of the flux density. Thereby, a sinusoidal flux density can be compared with the piecewise linear flux curve in a DAB3 application. In the following, these cases are referred to as sinusoidal and DAB3, respectively. In Figs. 3 and 4, the red solid graphs represent the DAB3, whereas the blue dashed graphs represent the sinusoidal excitation. Fig. 3(a) shows the reference magnetic flux density generated in core material, whereas Fig. 3(b) shows the voltage set by the test bench to achieve the reference flux. As expected, the voltage corresponds to the phase voltage in a DAB3. In a first comparison, Fig. 3(c) shows that the specific iron losses for DAB3 tend to be smaller, the area spanned by the hysteresis loop is smaller. Fig. 4 shows the measured specific iron losses as a function of the flux density. From that measurement, some data points are given separately in Table I, where $\hat{B}$ is the magnetic peak flux density and P_s are the specific iron losses in the material. The relative deviation is given as well. It is evident that the losses in a material for DAB3 are lower than those for sinusoidal excitation. As for equal peak flux densities, the maximum (dB/dt) for DAB3 is smaller compared with sinusoidal excitation, the specific iron losses are also smaller. In the following, the results are validated using a state-of-the-art analytical model.

IV. Analytical Validation

As the flux curves are nonsinusoidal but free from dc offsets, the improved generalized Steinmetz equation (iGSE) [8] is used to validate the core losses.

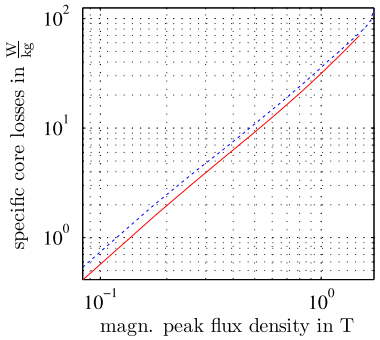

Fig. 4. Core losses for sinusoidal and piecewise linear course at $f = 1$ kHz.

TABLE I
Measured Specific Core Losses

$\hat{B}$ in T	Specific core losses in W/kg		Relative deviation
	$P_{s,sinus}$	$P_{s,DAB3}$	$\frac{\lvert P_{s,sinus} - P_{s,DAB3}\rvert}{P_{s,DAB3}}$
0.1	0.54	0.41	32 %
0.5	9.61	8.59	12 %
1.0	33.96	31.09	9 %
1.5	73.90	69.73	6 %

A. Derivation of the Steinmetz Parameters

The iGSE uses the Steinmetz parameters α, β, and k according to the original Steinmetz equation (OSE) [9]

$$P_s = k f^{\alpha} \hat{B}^{\beta} \quad \text{with} \quad [P_s] = \frac{\text{W}}{\text{kg}}. \tag{1}$$

To determine the Steinmetz parameters α, β, and k, the core losses P_s are measured for different frequencies and peak flux densities on sinusoidal excitation. The measurements are performed at the frequencies 1, 5, 7, and 10 kHz, the peak flux is varied from 0.1 to 1.8 T in steps of 0.1 T.

With the measuring results and (1), the Steinmetz parameters for silicon steel with a thickness of $d = 0.18$ mm are determined as follows:

$$\alpha = 1.6155 \qquad \beta = 1.7021 \qquad k = 5.2 \cdot 10^{-4}. \tag{2}$$

In Fig. 5, the measuring points are given, as well as the core losses calculated by the OSE using the above Steinmetz parameters.

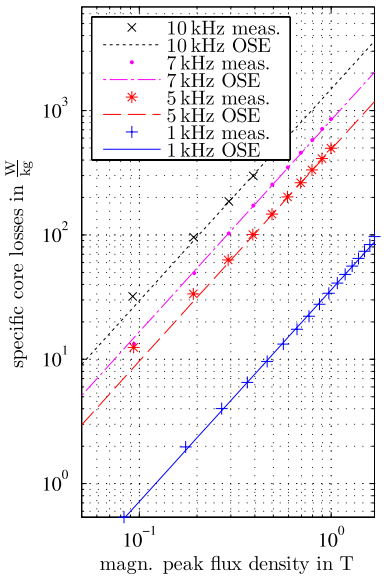

Fig. 5. Specific core losses in silicon steel for sinusoidal excitation.

B. Improved Generalized Steinmetz Equation

Equations (3) and (4) represent the well-known iGSEs, as published in [8]

$$P_s = \frac{k_i(\Delta B)^{\beta-\alpha}}{T}\int_0^T \left|\frac{dB}{dt}\right|^{\alpha} \mathrm{d}t \tag{3}$$

with

$$k_i = \frac{k}{(2\pi)^{\alpha-1}\int_0^{2\pi}|\cos\theta|^{\alpha}2^{\beta-\alpha}\mathrm{d}\theta} \tag{4}$$

where ΔB is the peak-to-peak value of the flux density, T is the period of the flux density, and α, β, and k are the Steinmetz parameters.

As also published in [8], for piecewise flux densities, (3) simplifies to

$$P_s = \frac{k_i(\Delta B)^{\beta-\alpha}}{T}\sum_m \left|\frac{B_{m+1}-B_m}{t_{m+1}-t_m}\right|^{\alpha}(t_{m+1}-t_m) \tag{5}$$

where (t_m, B_m) are the supporting points of the piecewise linear flux.

With the measured Steinmetz parameters given by (2) and (5), the iGSE has been used to calculate the losses for the piecewise linear flux. Fig. 6 shows the comparison of the measured core losses at sinusoidal and piecewise linear excitation with the results of the OSE and iGSE, respectively. The frequency is 1 kHz. While the results of the OSE are apparently in good accordance with the measuring, the iGSE slightly overestimates the losses of the piecewise linear flux course. Fig. 7 shows the difference between the measured core losses and the losses determined by the OSE and iGSE, respectively. It is evident that there is already in the OSE a slight uncertainty, which is propagated to the iGSE as the same Steinmetz parameters are used. This uncertainty might be related to the variation of the permeability for different flux densities and, in particular, the complex permeability of silicon steel at the evaluated frequencies [10]. Furthermore,

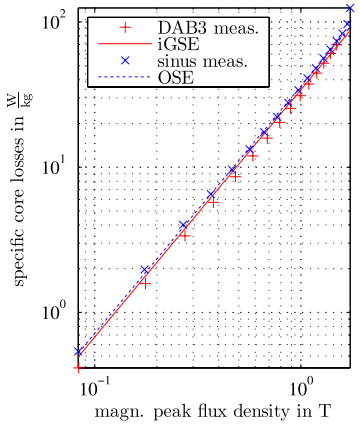

Fig. 6. Specific core losses for sinusoidal and piecewise linear course—measurement and iGSE.

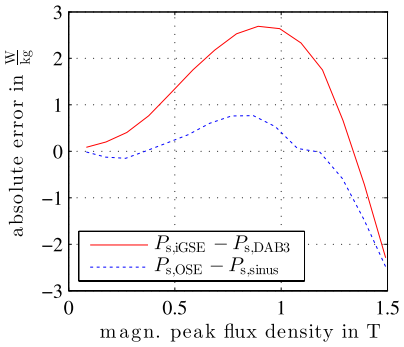

Fig. 7. Error between the measured losses and the one calculated by OSE and iGSE, respectively.

eddy currents occur at the given frequencies, which are not considered by the Steinmetz formulas [11].

However, as the relative error is sufficiently small, the iGSE delivers accurate core losses in a DAB3 application. The iGSE is used in the following to determine the core losses in a DAB3 under load.

V. DAB3 Under Load Condition

The previous investigation is based on a DAB3 operated in no-load condition. In the following, the core losses in a DAB3 under load are discussed.

To transfer power, a phase shift between the primary and secondary side transformer voltage is introduced by the power-electronic switches (Fig. 2). Both the primary and secondary side phase voltages generate a flux in the transformer core. These phase shifted fluxes superpose as also shown in Fig. 8. The actual peak flux under load $\hat{B}$ is smaller due to the superposition of the phase shifted fluxes. With increasing phase shift, the actual peak flux density $\hat{B}$ decreases. The maximal peak flux density at no load is referred to as $\hat{B}_0$ in the following.

The core losses under load are calculated using the iGSE. Therefore, magnetic relaxation during the phase of constant flux is not considered [12]. Fig. 9 shows the specific core losses in a DAB3 for different peak flux densities and loads, represented by the load angle. Note that even under load,

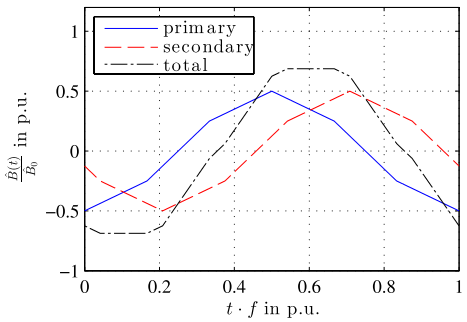

Fig. 8. Course of the magnetic flux density for a DAB3 under load condition ($\varphi = 75°$).

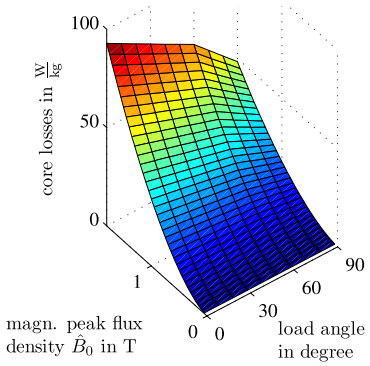

Fig. 9. Specific core losses in a DAB3 under load condition calculated by iGSE.

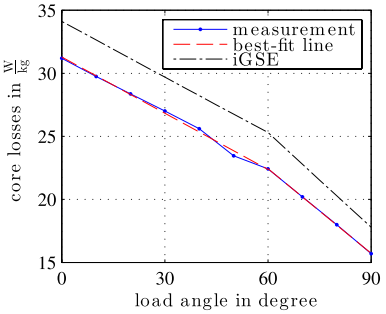

Fig. 10. Measured specific core losses in a DAB3 under load condition.

the losses are plot versus the corresponding no-load peak flux density $\hat{B}_0$. As the peak flux density $\hat{B}$ decreases with increasing load, the core losses decrease as well.

It can be seen in Fig. 9 that the core losses decrease faster for load angles beyond 60°. For load angles greater than 60°, the flux curves overlap in a way that the maximum (dB/dt) of the total flux is reduced compared with low-load conditions. As a consequence, the core losses decrease stronger. This effect has been validated through measurement. Fig. 10 shows the measuring results for $\hat{B}_0 = 1$ T. In this figure, two best fit lines are drawn. One is calculated from the measuring points in the interval [0°, 60°] and the other one from the points in the interval [60°, 90°]. The core losses calculated with the iGSE are given as well. There is a nearly constant error between measurement and iGSE that was also apparent in the no load measuring (Fig. 7). Apart from this offset, the measuring results are in good agreement with the iGSE. Therefore, the effect is verified in practice and should be considered when designing a DAB3 dc–dc converter.

VI. Conclusion

In the future, dc–dc converters will play a key role in the electric energy supply. The DAB3 is a perfect candidate for high-power dc–dc conversion. In this type of converter, the course of the magnetic flux density in the transformer is often approximated with a sinus. Thereby, the iron losses generated in the transformer are overestimated.

Measurements have shown that the actual power loss density is lower than the sinus approximation. From that measurements, the Steinmetz parameters of the 0.18 mm silicon steel sheets are determined. The iGSE is then used to validate the measurement of the actual piecewise linear flux course. The iGSE slightly overestimates the losses. Reasons for this might be the varying permeability of silicon steel and eddy currents at the evaluated frequencies.

The core losses in load condition of a DAB3 are analyzed using the iGSE. It is shown that for operation points $\varphi > 60°$, the core losses decrease as the maximal temporal derivative of the flux density is lower. This was verified through measurement.

References

[1] R. De Doncker, D. Divan, and M. Kheraluwala, "A three-phase soft-switched high-power-density DC/DC converter for high-power applications," *IEEE Trans. Ind. Appl.*, vol. 27, no. 1, pp. 63–73, Jan./Feb. 1991.

[2] R. Gonzalez, E. Gubia, J. Lopez, and L. Marroyo, "Transformerless single-phase multilevel-based photovoltaic inverter," *IEEE Trans. Ind. Electron.*, vol. 55, no. 7, pp. 2694–2702, Jul. 2008.

[3] M. Namikawa, H. Ninomiya, Y. Tanaka, and Y. Takada, "Magnetic properties of 6.5 % silicon steel sheets under PWM voltage excitation," *IEEE Trans. Magn.*, vol. 34, no. 4, pp. 1183–1185, Jul. 1998.

[4] J. Sagarduy, A. Moses, and F. Anayi, "Eddy current losses in electrical steels subjected to matrix and classical PWM excitation waveforms," *IEEE Trans. Magn.*, vol. 42, no. 10, pp. 2818–2820, Oct. 2006.

[5] H. Kaihara, N. Takahashi, M. Nakano, M. Kawabe, T. Nomiyama, A. Shiozaki, *et al.*, "Effect of carrier frequency and circuit resistance on iron loss of electrical steel sheet under single-phase full-bridge PWM inverter excitation," *IEEE Trans. Magn.*, vol. 48, no. 11, pp. 3454–3457, Nov. 2012.

[6] M. Kawabe, T. Nomiyama, A. Shiozaki, H. Kaihara, N. Takahashi, and M. Nakano, "Behavior of minor loop and iron loss under constant voltage type PWM inverter excitation," *IEEE Trans. Magn.*, vol. 48, no. 11, pp. 3458–3461, Nov. 2012.

[7] A. Boglietti, P. Ferraris, M. Lazzari, and F. Profumo, "Iron losses in magnetic materials with six-step and PWM inverter supply [induction motors]," *IEEE Trans. Magn.*, vol. 27, no. 6, pp. 5334–5336, Nov. 1991.

[8] K. Venkatachalam, C. Sullivan, T. Abdallah, and H. Tacca, "Accurate prediction of ferrite core loss with nonsinusoidal waveforms using only steinmetz parameters," in *Proc. IEEE Workshop Comput. Power Electron.*, Jun. 2002, pp. 36–41.

[9] C. P. Steinmetz, "On the law of hysteresis (Part II.) and other phenomena of the magnetic circuit," *Trans. Amer. Inst. Electr. Eng.*, vol. 9, no. 1, pp. 619–758, Jan. 1892.

[10] K. G. N. B. Abeywickrama, T. Daszczynski, Y. Serdyuk, and S. Gubanski, "Determination of complex permeability of silicon steel for use in high-frequency modeling of power transformers," *IEEE Trans. Magn.*, vol. 44, no. 4, pp. 438–444, Apr. 2008.

[11] M. Popescu, D. Ionel, A. Boglietti, A. Cavagnino, C. Cossar, and M. McGilp, "A general model for estimating the laminated steel losses under PWM voltage supply," *IEEE Trans. Ind. Appl.*, vol. 46, no. 4, pp. 1389–1396, Jul./Aug. 2010.

[12] J. Muhlethaler, J. Biela, J. Kolar, and A. Ecklebe, "Improved core loss calculation for magnetic components employed in power electronic system," in *Proc. IEEE 26th Annu. APEC*, Mar. 2011, pp. 1729–1736.